JOURNAL OF SPACECRAFT AND ROCKETS
Vol. 45, No. 4, July–August 2008

# Mechanical Actuators for Guidance of a Supersonic Projectile

K. C. Massey,* J. McMichael,† T. Warnock, and F. Hay‡
*Georgia Institute of Technology, Atlanta, Georgia 30332-0844*

DOI: 10.2514/1.31709

**In this paper, the results of a series of experiments to determine the feasibility of using small actuators to provide directional control for a supersonic projectile are presented. A method to control the flight of the projectile was proposed, which takes advantage of complex shock-boundary-layer interactions produced by mechanical devices. Experimental tests were conducted at the Georgia Tech Research Institute in a supersonic wind tunnel to screen actuator locations, and these tests provided insights into the best actuator locations and force levels that were found to be large enough to produce high *g* turns on a notional projectile. Further experiments were conducted on a scale projectile to measure the moment produced on a notional Mach 4 projectile. Several different mechanical actuators were tested, which served to provide guidance for future actuator designs. Computational fluid dynamics results were also used to predict the results in flight. It was found that the forces predicted by the computational fluid dynamics and measured by the experiments were quite close, which lends credence to both methods. The results from the experimental and numerical efforts were used to design test articles that were successfully fired at an Army Research Lab test range.**

## Nomenclature

$M$ = Mach number
$P$ = pressure
$X$ = distance in streamwise direction along fin
$Y$ = distance perpendicular to face of fin

## I. Introduction

THERE has been recent interest in both missiles and guided projectiles that operate in the high supersonic to hypersonic range for various missions. The Office of Naval Research has been pursuing HyFly [1], which is a proposed Mach 6 missile that would be used to strike targets of opportunity in a timely fashion before they could reposition. Marx et al. [2] discuss small guided projectiles that are under consideration for the future objective force. They discuss how the increased lethality of guided projectiles will improve the survivability of the future soldier. Another area of interest revolves around cruise missile defense, such as the Defense Advanced Research Projects Agency's (DARPA's) Low Cost Cruise Missile Defense program and the U.S. Army's Enhanced Area Air Defense System. One possible scheme for missile defense assumes that medium caliber guns with high rates of fire could fire multiple supersonic projectiles that could be guided into an incoming missile that may be undergoing evasive action. Warnash and Killen [3] describe several military programs in which high-speed guided munitions are in development or are under consideration. In all cases, it is found that the high closure rates between the projectile and the target may necessitate large turning forces.

It was the goal of this effort to provide an initial feasibility study into the use of strategically located actuators to provide the turning force needed to terminally steer a missile or projectile. Initially, only jet actuators were considered. These jets were not intended to be simple reaction jets, but were intended to modify the flow around the projectile in such a way as to greatly enhance the force on the body of the projectile. As the research progressed, the use of deployable pins was also evaluated to generate turning forces. Efforts were made to understand the physics behind these turning forces so that the lessons learned here could be applied to future missile and projectile geometries.

Experimental studies that involve jets in supersonic cross flows have been pursued for nearly 60 years and, thus, there are too many works to cite here. Margason [4] provides an excellent review of many of the experimental studies. Spaid and Cassel [5] examine the particular case of aerodynamic interference induced by reaction controls and correlate the pertinent experimental data over a wide range of Mach numbers and Reynolds numbers. As pointed out by Hemsch [6] and by Hsia [7], the basic fluid dynamic interactions of a solid body, or a jet, in a supersonic crossflow are essentially the same, as a jet provides blockage to the flow. In both cases, the influence of the jet, or solid object, is felt upstream due to a thickening of the boundary layer. This is shown in Fig. 1, in which the upper sketch shows how the thickening of the boundary layer leads to an upstream separation shock and a downstream recirculation zone. In the lower portion of Fig. 1, the pressure field associated with this disturbance is shown. Upstream there is a rise in pressure associated with the shock, whereas downstream there is a low-pressure region associated with the recirculation zone. The ratio of the rise in pressure was shown by Spaid and Cassel [5] to collapse as a function of Mach number, as shown in Fig. 2 for Mach numbers from 1.5 to 13. Spaid and Cassel also showed that the geometric extent of the pressure disturbance could also be collapsed with appropriate Mach number scaling. Although all of these experimental results were for a flat plate, they demonstrate that the pressure disturbances generated at one flight condition can be related to those of another flight condition through appropriate scaling.

Much of the initial work on jets in a crossflow was done in the 1960s and 1970s and was related to reaction control jets (RCJs) on missiles and ballistic vehicles. The nature of these studies was to examine the impact of RCJs on the overall flowfield around the body. One of the more interesting works in this field was by Champigny and Lacau [8], in which many different parameters of RCJs were experimentally explored. Variations such as the pressure ratio, gas temperature, injection port geometry, injection port orientation, injection port location, flight Mach number, and other permutations were explored. Of particular relevance to the present study, they showed that the effect of the RCJ location relative to the missile fins strongly affected the missile pitching moment.

Presented as Paper 4970 at the 23rd AIAA Applied Aerodynamics Conference, Toronto, Ontario, 6–9 June 2005; received 1 September 2007; revision received 28 December 2007; accepted for publication 5 January 2008. 

*Senior Research Engineer, Aerospace Transportation Advanced Systems Lab, Georgia Tech Research Institute. Associate Fellow AIAA.
†Lab Director, Aerospace Transportation Advanced Systems Laboratory, Georgia Tech Research Institute. Associate Fellow AIAA.
‡Student, School of Aerospace Engineering. Student Member AIAA.

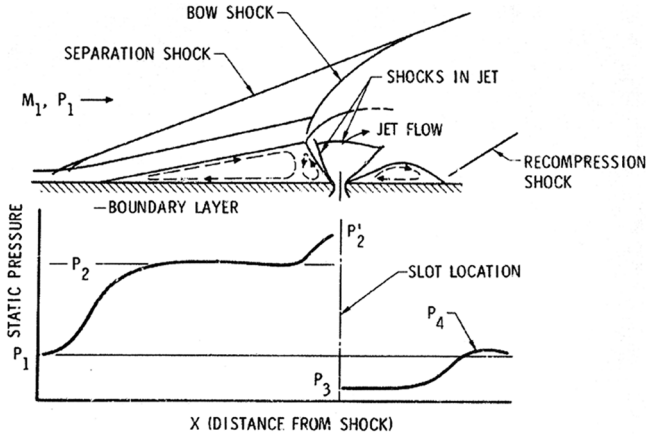


**Fig. 1 Flowfield and pressure distribution of a supersonic jet in a supersonic cross flow (Spaid and Cassel [5]).**

Recent work has focused both on the mixing phenomena associated with jets in regard to developing supersonic combustors and in maneuvering projectiles. Much of the more recent work with regard to jets in a crossflow has been numerical in nature, such as that of Schetz [9] and Fujimori [10]. The effects of different gas densities, such as injecting hydrogen into air, have also been explored by Takahashi and Hayashi [11] and others. Several recent research efforts on maneuvering projectiles, such as the UK HOTLiP program [12] and Army Research Lab efforts, have also been numerical in nature. Graham and Weinacht validated their numerical scheme to predict a control jet interaction [13] and then, with Brandeis, used their method to examine the case of a finned projectile with control jets [14]. They demonstrated that there were significant interactions that could increase the aerodynamic pitching moments relative to the jet thrust alone.

In the fall of 2001, the Georgia Tech Research Institute (GTRI) initiated a DARPA-funded study to investigate the feasibility of using our flow control expertise to develop techniques capable of enabling a supersonic projectile to undergo rapid maneuvers. Based on the authors' experience and the available literature, the program attempted to develop jet actuators that would not rely solely on the thrust of a jet-based actuator but would obtain a high force multiplier through aerodynamically influencing the flow around the body. The interactions between a jet and supersonic flow were fairly well understood, yet the influence on the aerodynamic characteristics of a missile or projectile were not. Previous work had shown that aerodynamic interactions between RCJs and the body could influence the pitching moments and lift in either a positive or negative fashion, but this work was very limited in scope. In the public literature, it appeared that few efforts had been made to design for a favorable jet interaction that would amplify the force input. It thus became the objective of this study to design such a system in which an actuator could rapidly influence the flowfield around the missile or projectile to generate the forces needed to rapidly turn the body.

To further evaluate this concept, a series of experiments and numerical studies were conducted. The wind-tunnel tests, conducted at GTRI, consisted of both a series of screening tests to determine if sufficient forces could be generated and where to place the actuators and more representative tests to measure moments and determine the rise time of the forces produced. These experimental tests were complemented by computational fluid dynamics (CFD) to better understand the fluid mechanics and to measure quantities not easily measured in the lab. These methods were compared to provide additional validation.

## II. Pin Fin Concept and Experimental Evaluation

### A. Concept

Based on the lessons learned in previous efforts, a concept was developed to increase the force produced by properly locating the actuator. Building on the fact that the flow disturbance introduced by a jet or solid object inserted into the flow was three dimensional in nature and extended away from the body of the projectile, it was hypothesized that if the actuator was moved close to a fin, not only would there be regions of high pressure generated on the body, but also on the fin as well. This is shown conceptually in Fig. 3, in which a shock is created by an interaction between two pins and the flow. (Prior experiments had also shown that the use of pins was superior to that of jets, particularly in the small form factor of a projectile.) In this conceptual image, the shock also has a large interaction with the fin

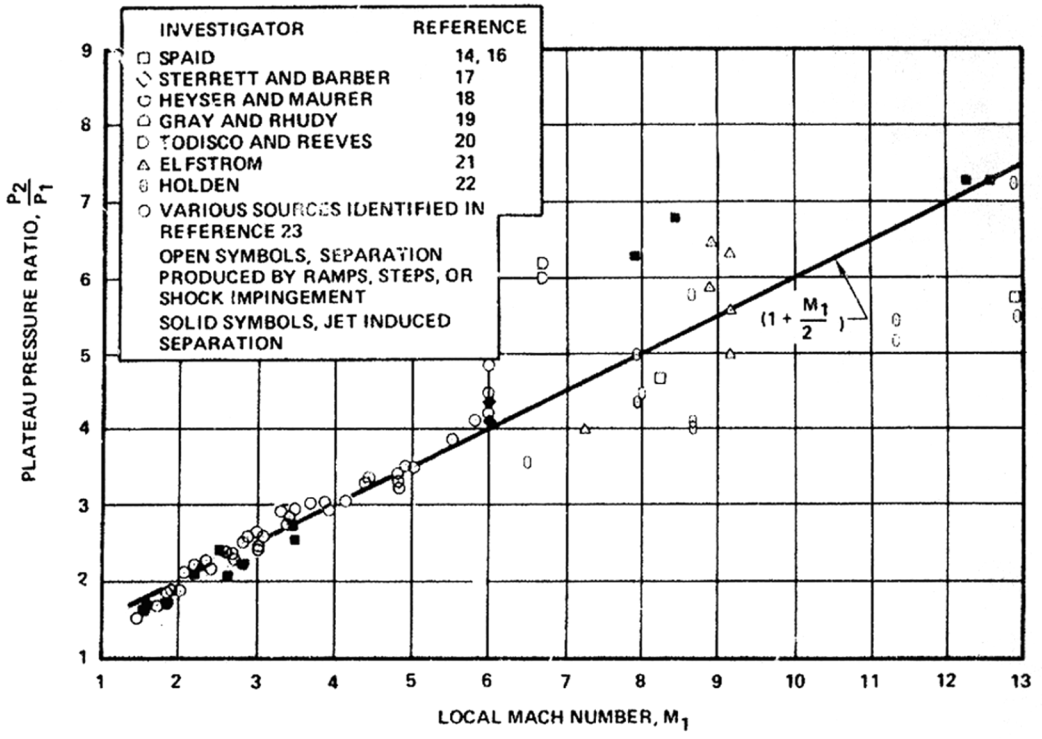


**Fig. 2 Correlation of the plateau pressure rise with the local Mach number (Spaid and Cassel [5]).**

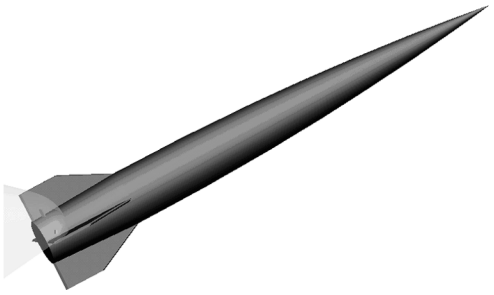

**Fig. 3 Pin fin concept.**

as well as the body. Taking advantage of this 3-D corner effect should enlarge the surface area of the projectile experiencing high pressure relative to positioning the actuator further away from the fins. One advantage to this concept is the fact that generating forces on the surfaces of the fins allows one to also control the roll rate of the projectile or missile. This enables the pursuit of different control schemes that might not have otherwise been possible.

### B. Test Setup

To validate this concept, a series of experimental tests and numerical studies were conducted. The first experimental tests used a simplified representative geometry that consisted of a fin on a flat plat immersed in a supersonic stream. The jet was a convergent divergent jet that could be operated at Mach 1.7 in a nearly shock-free fashion to produce the freestream flow. The air for this jet (and subsequent jets) was supplied from an underground reservoir of clean dry air stored at 20°C and 2 MPa, and the jet was expanded to atmospheric pressure. The fin was mounted onto a disk that could be rotated to change the angle of attack (AOA) of the fin relative to the stream. A picture of this hardware mounted into GTRI's Hot Jet Facility is shown in Fig. 4. The fin was designed to maximize its size while still allowing it to be immersed in the jet. As seen in Fig. 5, the fin was 1.5 in. tall and 3 in. long. The fin was instrumented with 18 pressure taps that were cut into the fin using a wire electrical discharge machining process. The pressures measured from these pressure ports were used to estimate the force on the fin by assuming a constant pressure in the vicinity of the pressure ports. A series of seven holes where pins ($\frac{1}{4}$–20 bolts) could be raised and lowered were tapped into the ground plane for a crude first approximation. The physical locations of these holes relative to the fin are shown in Fig. 6, in which the reference number for each hole is also shown.

All of the pressures from the pressure ports were read simultaneously using at a sampling rate of approximately 10 Hz. These pressures were averaged over the course of 3 s using 30 samples. Each of the averaged pressure values was associated with a given area and, thus, the forces on these areas (shown in Fig. 7) could be calculated. Summing up these forces led to an estimation of the force on the fin. Note that only the surfaces parallel with the stream were used in these calculations, as it was not feasible to measure the pressures on the tapered parts of the fin. Contour plots of the pressures on the instrumented surface of the fin were also generated, as shown in Fig. 8.

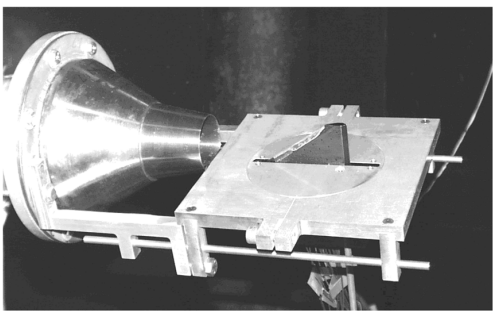

**Fig. 4 Installed hardware of fin interaction experiment.**

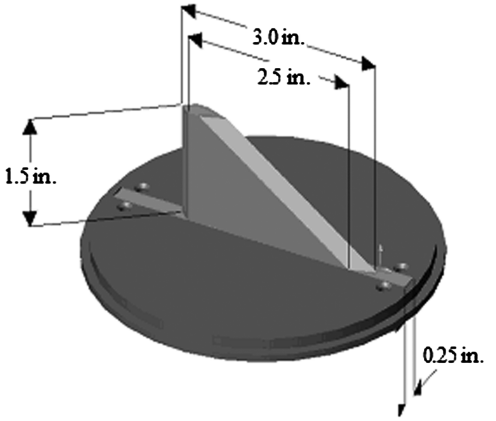


**Fig. 5 Dimensions of the experimental fin.**

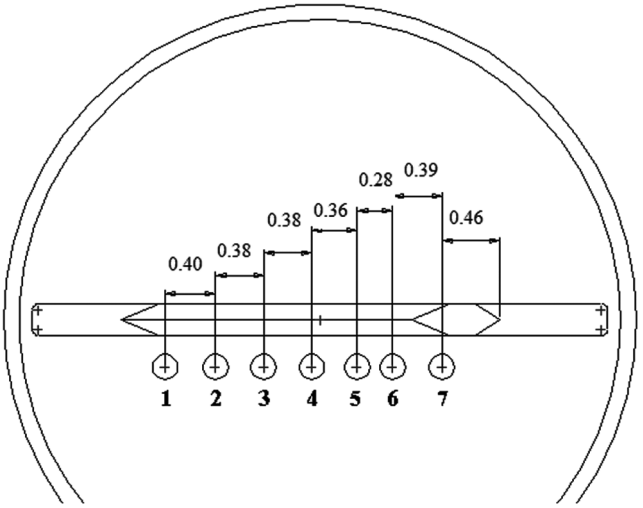


**Fig. 6 Dimensional spacing of pins and hole reference numbers.**

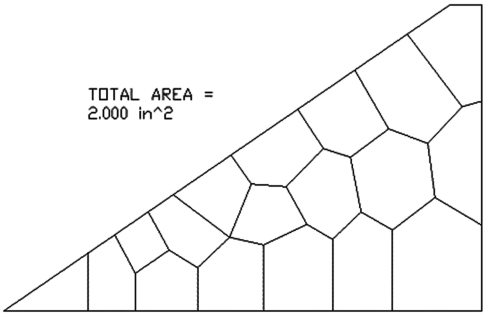


**Fig. 7 Pressure port layout and associated areas for the experimental fin.**

The $\frac{1}{4}$–20 bolts allowed for rapid testing to determine the optimal streamwise location of the actuators as well as the penetration depth of the jet or pin that would be required. A series of tests were conducted in which the pins were raised to three different heights at each of the seven hole locations. Pressure data were recorded for each of these runs. To ensure that there was no effect on the other side of the fin, these tests were repeated with a mirror image set of holes on the other side of the fin. Measurements were made for three different pin insertion depths, 1 diameter, 2 diameters, and 2.4 diameters, at all of the hole locations. Only a limited set of the data is shown here.

### C. Flat Plate Fin Results: Part I

At the minimum insertion depth of 1 diameter, large changes were induced in the flowfield which in turn drastically changed the

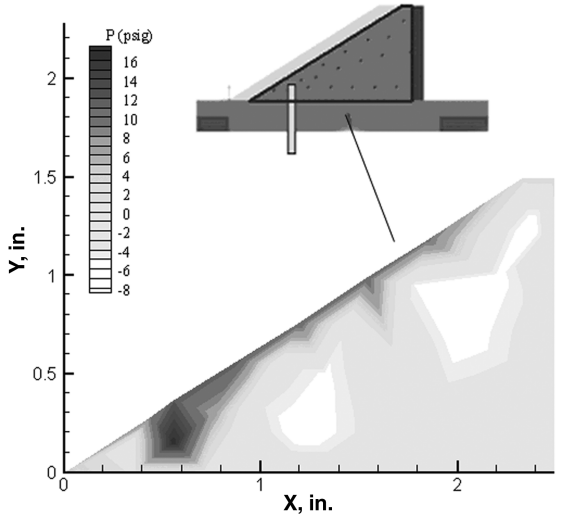


**Fig. 8 Generation of pressure contours on the fin from experimental data.**

pressures on the fin. As anticipated, these pressure fields were characterized by a pressure increase in the vicinity of the pin and a downstream region of low pressure. These effects are shown quite clearly in Fig. 9, in which the pressure levels on the fin when a pin was inserted at hole 2 are shown. For this case, the pressure change due to the presence of the pin resulted in a net drop in pressure over the entire fin. Although there was a pressure increase near the pin, the low-pressure region downstream covers a larger area resulting in a net suction force of about 1 lb. One can also clearly see that the pressure changes are three dimensional in nature as virtually the entire fin is affected.

At pin positions further downstream, the pressure changes on the fin have essentially the same character with the pressure changes shifted downstream. With the pin at hole 4 (see Fig. 10), it is clearly seen that the low-pressure region occurs further downstream than when the pin was at hole 2. The pressure forces on the pin are roughly of the same magnitude for both holes 2 and 4, but the sum force is

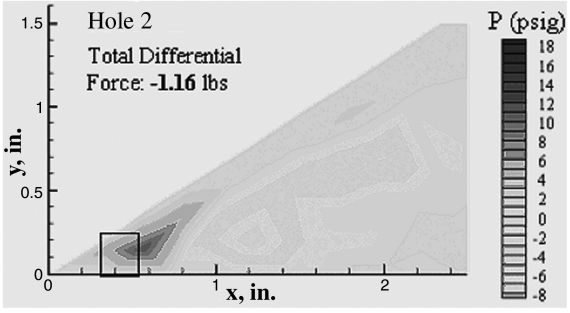


**Fig. 9 Fin pressure for the 1-diam height at hole 2.**

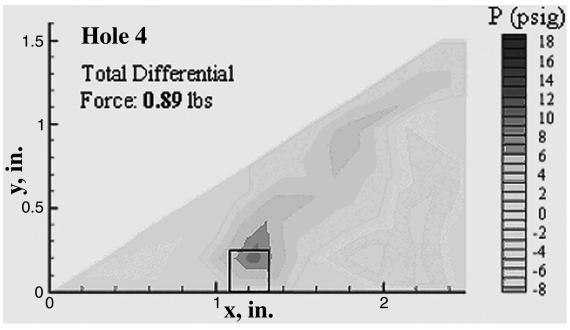


**Fig. 10 Fin pressure for the 1-diam height at hole 4.**

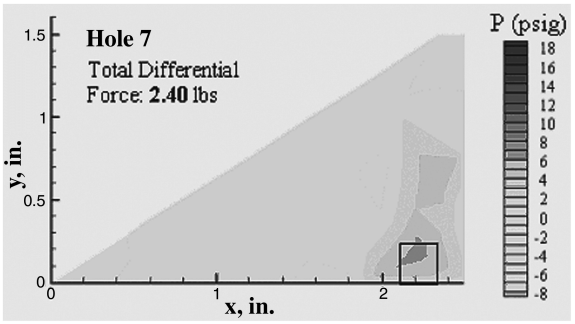


**Fig. 11 Fin pressure for the 1-diam height at hole 7.**

positive for hole 4 whereas it is negative for hole 2. This is due to the fact that the fin sees less of the low-pressure region behind the pin. Figure 11 shows that this is even more evident when the pin is at hole 7, where the low-pressure region is not even felt by the fin. As would be expected, the pressure force is even higher for this case and was found to be 2.4 lb. A summary of the forces induced by a pin inserted to a height of 1 diameter is shown in Fig. 12. It is clear that the force is maximized as one moves the pin downstream, thus eliminating the effects of the downstream separation.

When the height of the pin was increased to 2 diameters, pressure changes on the fin were dramatically increased. These changes suggest that the shock structure was much stronger and produced both larger changes in pressure on the fin and increased the area affected by the shock interactions. In Fig. 13, data are shown for a 2-diam-height pin at hole 2. Here it is seen that for the high-pressure region the peak differential pressure is higher and that the low-pressure region has lower pressures than for the corresponding 1-diam-height pin in Fig. 9. As a result, the total force on the fin is increased by roughly a factor of 3 to 3 lbs. In Fig. 14, which shows the data for the 2-diam-height pin at hole 7, it is seen that the extent of the pressure change is larger than for the 1-diam height. For the 2-diam-height case, the pressure disturbance nearly extends to the top of the fin, and it is thus likely that greatly increasing the pin height would provide diminishing returns in terms of increasing the force on the fin.

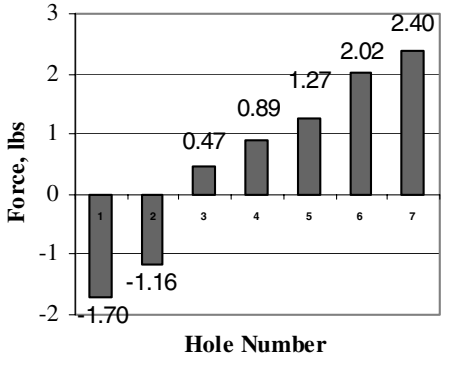


**Fig. 12 Differential forces for a 1-diam-height pin for various pin locations.**

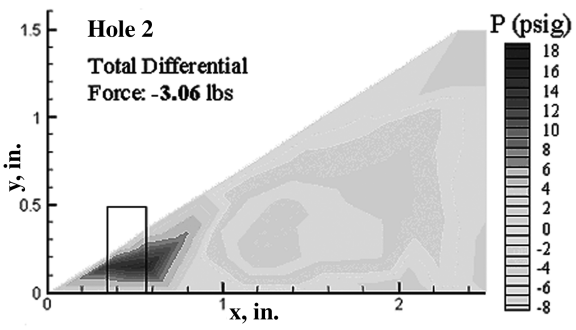


**Fig. 13 Fin pressure for the 2-diam height at hole 2.**

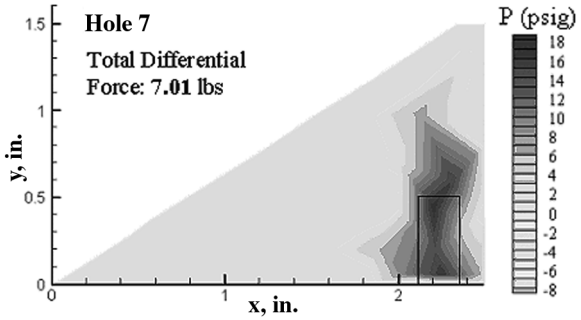


**Fig. 14 Fin pressure for the 2-diam height at hole 7.**

Further measurements were made using a slotted jet instead of the crude pins, with similar force contours. The data are not presented here as the contours are very similar. Essentially the same pressure forces could be generated with a jet that introduced the same level of flow disturbance as the pins. This, however, requires high pressures and exceedingly high mass flows as the Mach number of the freestream increases. For this reason, it was felt that the use of jets as opposed to mechanical pins did not make sense for a relatively small projectile.

As the force generation was intended to be used for maneuvering a finned projectile, the fins would be at some angle of attack at some point during the maneuver. Experiments were thus conducted with the fins at various angles of attack relative to the flow. It was found that the forces on the fin were diminished with an increasing angle of attack but only slightly. Using the 2-diam-height pin at hole 7 as a baseline, pressure data were acquired for two other angles of attack. At a 3-deg angle of attack, the total force was reduced from 7.01 to 6.66 lb. It appeared that the localized region of very high pressure near the pin may be smeared out a little more, but that the larger region of high pressure did not extend as far forward at the angle of attack. These observations are more evident at a 5-deg angle of attack, as the force level saw a further reduction to 6.38 lb. Nevertheless, the force levels at the angle of attack still remained substantial.

### D. Flat Plate Fin Results: Part II

After analyzing the results from the initial flat plate fin tests, it was decided to pursue the use of pins as actuators over jets. Several design changes were made and implemented in an effort to both improve the fidelity of the measured results and to further optimize the pin location.

Much of the same hardware was used as in the previous tests, but modifications were made to the flat plate that allowed for the pin to be moved both in the streamwise direction and normal to the fin direction. Because a rough optimal streamwise location was found in the previous tests, it was possible to fine tune the adjustability in this direction. This setup, which is shown in Fig. 15, also allowed for the pin to be rotated. Although this setup did not allow for infinite variability, it did allow us to further hone in on the optimal pin location and angle.

It was also felt that other pin geometries besides round pins could produce more force on the fin. In addition, these nonround shapes might also produce a complementary force in the desired direction. Four different pins were tested in these experiments. Their cross-sectional shapes are shown in Fig. 16. The trapezoid shape was conceived in the hope of generating a complementary force on the pin. The flat plate, or flap pin, was tested to mimic the deflection of a flap near the trailing edge of the fin. The two round geometries were tested to provide some continuity with the previous tests and to verify if any benefits were actually achieved with the nonround pins.

Before making the experiments described in Sec. II.C, it was not known where on the fin would be the regions of high induced pressure. From these earlier experiments, it was known that the fidelity of the measurements could be improved if additional pressure ports were added in the vicinity of the pin. An additional 10 pressure taps were added to the fin in this region for the next set of

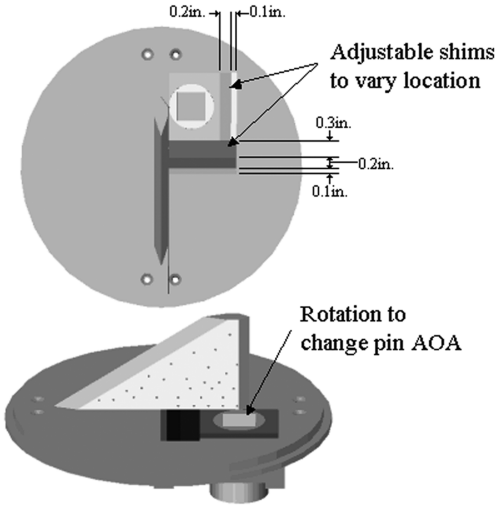


**Fig. 15 Second-generation fin flat plate experimental setup.**

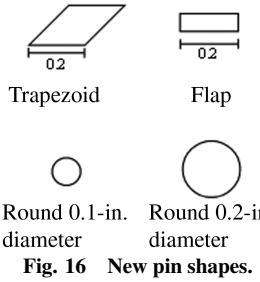


**Fig. 16 New pin shapes.**

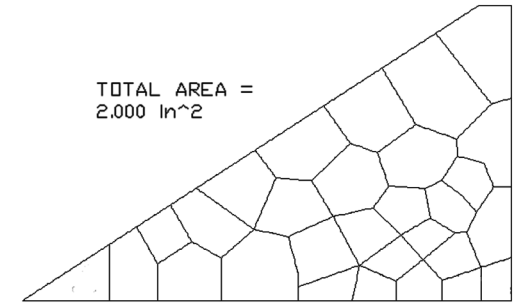


**Fig. 17 Second-generation pressure port layout.**

experiments. In Fig. 17, the new layout of the pressure ports can be seen. Comparing this layout with that of Fig. 7, the areas where pressure is assumed to be constant have been greatly reduced in the area where the largest pressure changes are expected. This change clearly results in an increased fidelity in the force calculations.

A picture of the trapezoid pin installed next to the modified fin and flat plate is shown in Fig. 18. Here it is possible to distinguish the new pressure taps added to the fin as the lighter-colored holes. (They are lighter in color because the fin was not anodized after drilling the new holes.) The spacing plates and rotation mechanism for the pin can also be seen. Some feel can also be gained of the height of the pin relative to the fin. For all of these experiments, the pin height was set to 0.5 in., which was nominally 2.5 times the longest dimension of the pin.

Two of the pressure contours from the round pin results are shown in Figs. 19 and 20 for the 0.1- and 0.2-in.-diam round pins, respectively. Qualitatively, they both resemble the results for the $\frac{1}{4}$-20 pins at a similar location shown in Fig. 14, and the force levels are similar for the 0.2-in.-diam pin. It is interesting to note that the peak pressure amplitudes are greater for the smaller diameter pin, as shown in Fig. 19, even though the overall force is 50% higher for the larger pin. This typifies the result that it is more important to influence a larger area of the fin, as shown in Fig. 20.

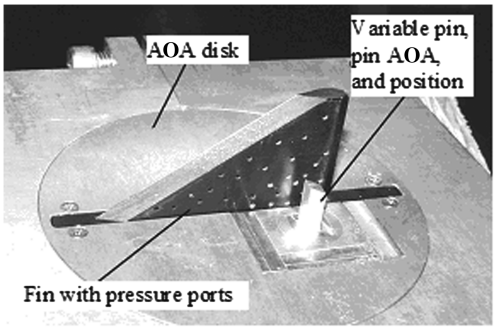


**Fig. 18 Experimental setup for the pin shape and the optimization of pin location testing.**

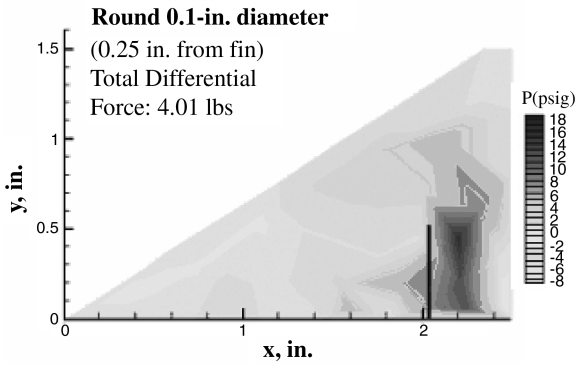


**Fig. 19 Fin pressure induced by the 0.1-in.-diam, 0.5-in.-height round pin at 0.6 in. from the trailing edge (TE).**

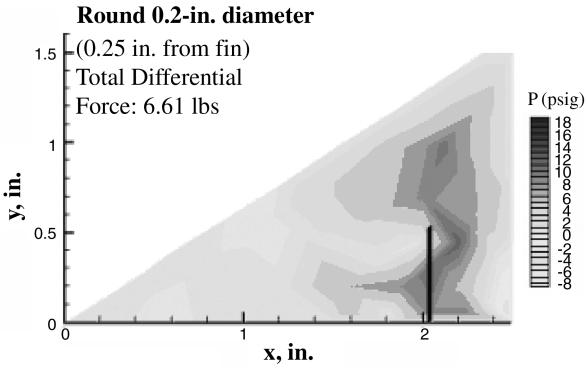


**Fig. 20 Fin pressure induced by the 0.2-in.-diam, 0.5-in.-height round pin at 0.6 in. from the TE.**

Detailed studies into the optimal location and angle of the nonround pins were performed. The effect of the angle of attack of the pin on the fin side force for both the flat and trapezoidal pins was measured over a range of angles. For these measurements, a 0-deg angle of attack represented the case in which the pin was oriented as shown in Fig. 16 and the flow was moving from the top to the bottom of the page. For a positive angle of attack, the pin was rotated counterclockwise. Figure 21 shows the effect of the pin orientation on the pressure force exerted on the fin. The pin orientation does not have a very strong effect on the flat pin, whereas for the trapezoidal pin the force can vary by a factor of 2 depending on the orientation of the pin. Effectively, the rotation of the pin resulted in a change in the pin frontal area presented to the flow. It is hypothesized that it is this frontal area that drives the flow disturbance, which in turn drives the amount of force produced on the fin. For the trapezoid pin, an angle of attack of $-30$ deg was near the optimum orientation for force generation and, thus, this orientation was used for the remaining tests to optimize the pin location.

The previous efforts with the $\frac{1}{4}$-20 pins clearly demonstrated that the force level was increased as the pin was moved closer to the

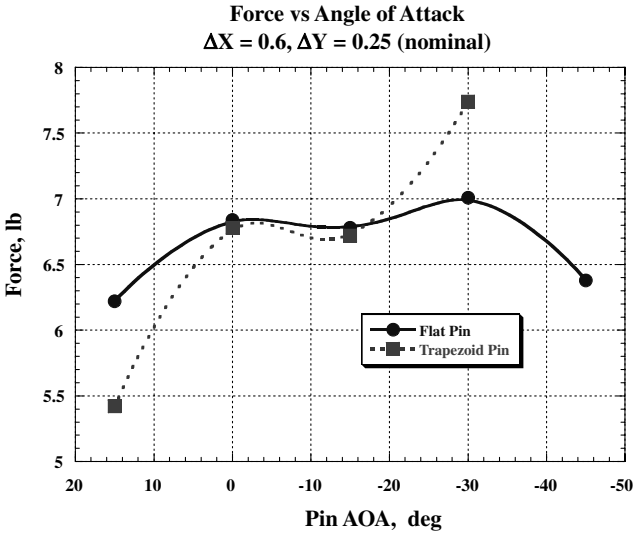


**Fig. 21 Effect of the pin angle of attack on the pressure force generated on the fin.**

trailing edge of the fin. This increase in the force was found to be due to the fact that the low-pressure region found downstream of the pin would occur off the body. Because similar results were expected for the nonround pins, the search range for the optimal pin location was narrowed. In Fig. 22, the force levels for the round (prior results), trapezoidal, and flat pins are shown as a function of the distance from the fin trailing edge for a fixed pin height and separation distance from the fin. Although the optimal location appears to vary slightly for the flat pin and the trapezoidal pin, in both cases it is near 0.65 in. from the trailing edge. It is possible that this is also the optimal location for the round pin as well, though the data are too coarse to be positive.

The separation distance for the flat pin from the fin was found to strongly affect the force generated. As seen in Fig. 23, the force levels varied by a factor of 4 for the flat pin. For the trapezoidal pin, the force induced on the fin did not change noticeably as the pin was moved from 0.15 in. from the fin to 0.25 in.; however, it rolled off rapidly for further separation. For the flat pin, there was a noticeable change in both the total forces and the pressure contours as the pin was moved perpendicularly away from the fin. In Fig. 24, the flat pin is 0.25 in. from the fin whereas in Fig. 25, the pin has been moved closer to 0.15 in.

The second set of experiments testing a pin in proximity to a fin on a flat plate demonstrated that the force level produced by pins could be augmented by the appropriate placement and orientation of a

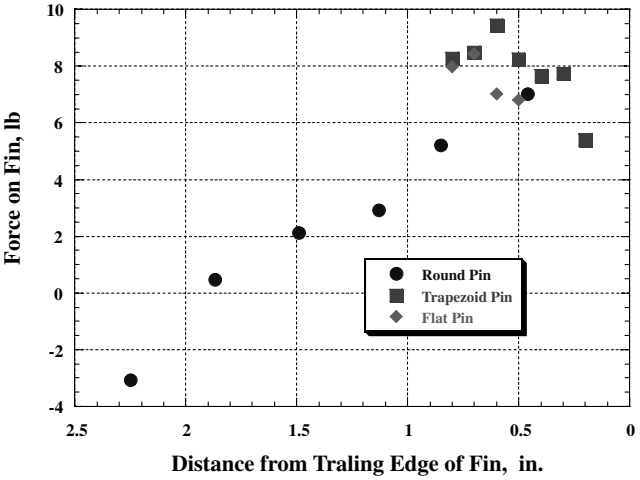


**Fig. 22 Effect of distance from the trailing edge on the force produced by the pins.**

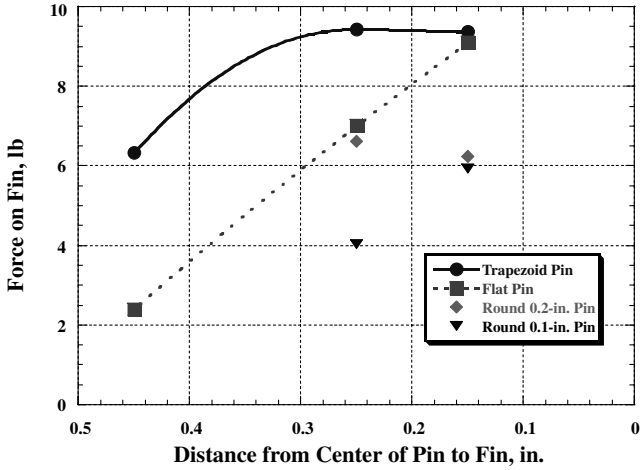


**Fig. 23 Effect of distance from the fin on the force generated by the various pins.**

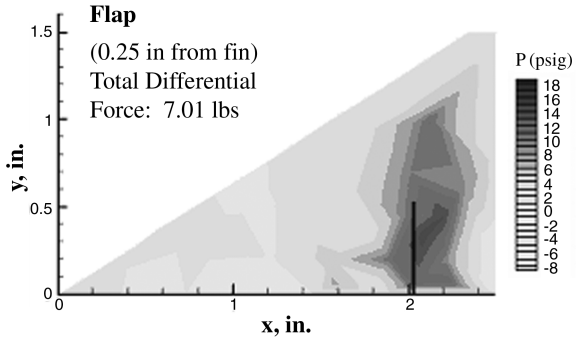


**Fig. 24 Fin differential pressure induced by the 0.5-in.-height flat pin at 0.6 in. from the TE.**

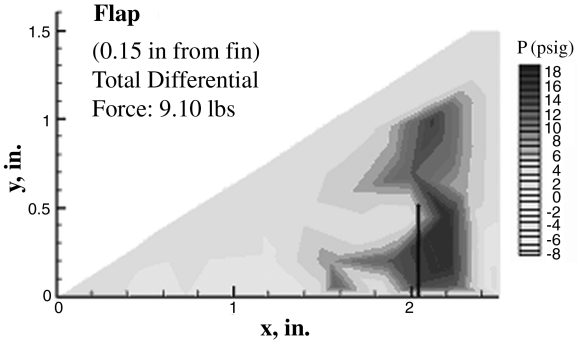


**Fig. 25 Fin differential pressure induced by the 0.5-in.-height flat pin at 0.6 in. from the TE.**

nonround pin. The use of nonround pins resulted in force levels that were 50% higher than for round pins. It was also shown that the streamwise location of a pin for maximum force generation was independent of the geometries tested. The results demonstrated that the force levels had a strong dependence upon the separation between the pin and the fin. There was some evidence that the force levels were reduced as portions of the pin entered the boundary layer of the fin. The orientation of the pins was also shown by the experiments to introduce changes in the force level on the fin. A third set of experiments involving a flat plate and fin was conducted using a force balance and a further refined set of pins, as described by Hay and Massey [15]. The experimental results were very useful in optimizing the location of the pins; however, they were lacking in predicting the total forces and moments that would be developed on a projectile. For that reason, further CFD studies were conducted.

## III. CFD of Pins

Numerical simulations of the flow over a projectile with pins in both a roll control configuration, Fig. 26, and a directional control configuration, Fig. 27, were conducted. For a single Mach number, both flat and trapezoidal pins were studied for a projectile at several small angles of attack. The orientation and the location of the pins were based on the aforementioned experimental results. For this orientation of the pins, the trapezoidal pin has roughly 1.7 times the frontal area of the flat pin and thus generates more force. The surface pressures generated on the fin, pin, and body for the flat pin are shown in Fig. 28. Here the high pressures generated by an upstream shock similar in nature to that conceptualized in Fig. 3 are apparent. The region of increased pressure extends upstream to nearly three-fourths of the fin height. Near the trailing edge of the body/fin juncture, a small region of low pressure exists due to separation behind the pin. It was desired to have this region completely off the body and, although this is mostly achieved, it might be possible to further optimize the location. For the same flow conditions, the pressure distribution for the trapezoidal pin configuration is shown in Fig. 29. For the most part, the pressure contours are quite similar between the two different geometries. However, it is possible to see that the region of increased pressure both extends further and is stronger for the trapezoid pin. The high-pressure region extends all the way to the opposite fin for the trapezoid pin. On the other hand, the region of low pressure behind the pins is also more pronounced for the trapezoidal pin. In both cases, there are extremely high pressures on both of the pins that will obviously result in increased drag. These high pressures are complemented by very low pressures on the leeward side of the pins. For a properly designed and oriented pin, it may be possible to take advantage of this situation to generate forces in a chosen direction.

The rolling moments predicted by the CFD were quite large, as the pins were sized more for directional control than roll control. With rolling moments of approximately 0.25 $N \cdot m$, the calculated angular roll rate accelerations are on the order of 4000 $rad/s^2$ assuming no

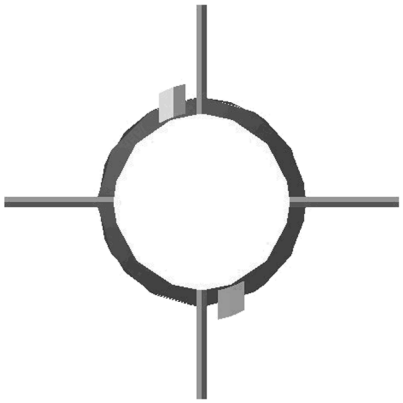

**Fig. 26 Pins used for roll control.**

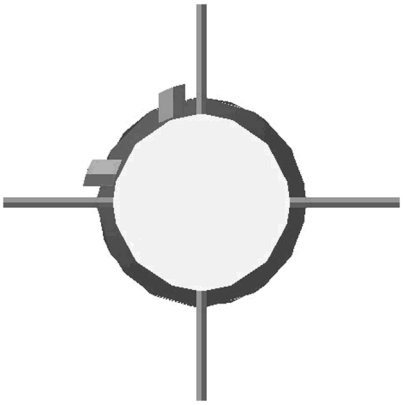

**Fig. 27 Pins used for directional control.**

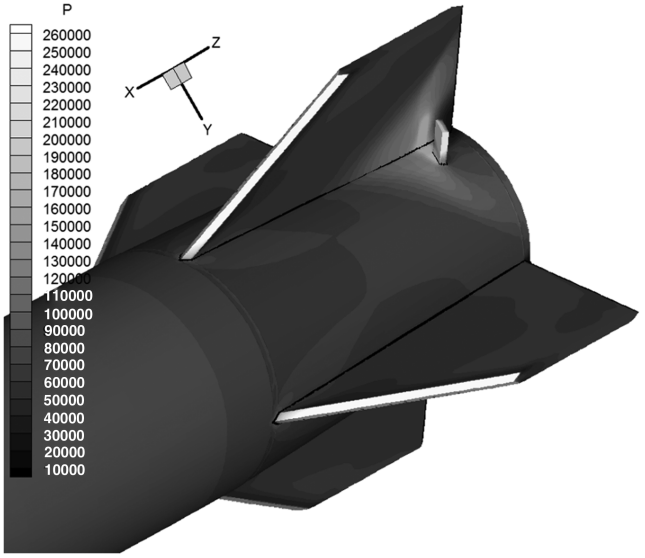


**Fig. 28 Surface pressures for the flat pin with the projectile at zero angle of attack, roll control configuration.**

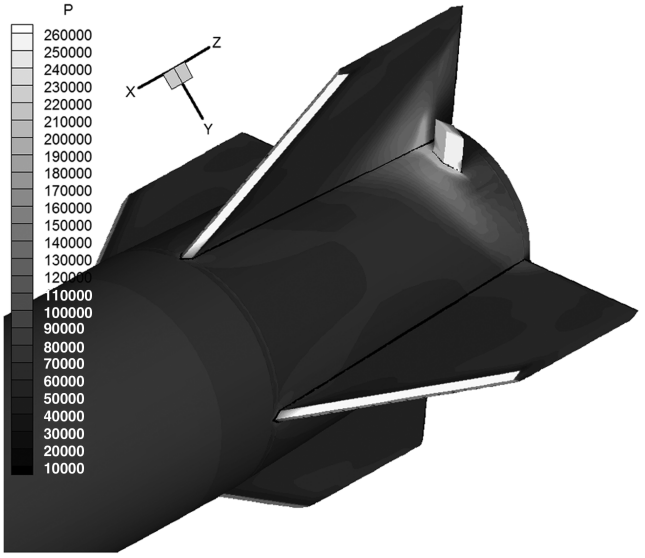


**Fig. 29 Surface pressures for the trapezoid pin with projectile at zero angle of attack, roll control configuration.**

aerodynamic forces and an axial moment of inertia of 580 $g \cdot cm^2$. This level of roll torque was later demonstrated on a gun range at the Aeronautical Research Laboratory (ARL) to produce roll rates such that the projectile could be rolled 180 deg in 13 ms [16]. Rapid roll control schemes can thus be developed using these control pins.

Using the results from the CFD, it was possible to conclude that the use of pins could conceptually produce enough force and moment to implement a bank to turn type control scheme. Subsequent 6-degree-of-freedom simulations based on the results described in this paper implanting such a concept are described in Massey et al. [17]. Several hurdles still remained, including the mechanization of the control pins, the measurement of forces on a more flight representative platform, and the measurement of time response of the forces in relation to pin deployment.

## IV. Scale Model Tests

Another series of experiments were conducted at GTRI involving the measurement of forces and moments on a scale model in a supersonic stream. There were three main goals of these tests: to determine the effect of pin height on force and moment, to estimate system response time, and to develop new ideas for how to package the system for final use. Steady force and moment measurements were made for a range of pin heights and orientations to determine their effect on force and moment. In addition, dynamic force measurements were made as an actuator was deployed and, although these results are omitted for the sake of brevity in this paper, further details can be found in Massey et al. [18].

### A. Scale Model Hardware and Setup

To measure the forces and moment introduced by a pin on the projectile under investigation, an experiment was designed in which the full projectile was modeled as a full-scale half projectile on a ground plane. The projectile was split along a longitudinal line of symmetry that split two fins. This split line was chosen due to the constraints imposed by the 1 translational degree of freedom of the force balance.

A Mach 2.5 convergent/divergent nozzle was designed and fabricated to create the supersonic stream over the projectile. The exit area of this nozzle was 3 by 1 in. The nozzle was supplied compressed and dried air at 300 psi that was regulated by a 4-in. valve. A top view of the nozzle, ground plane, and projectile is shown in Fig. 30. A view from the other side of the test assembly, Fig. 31, shows additional details such as the moment arm and the sensor used to measure moment as well as the pressure transducer to set the nozzle pressure ratio and the signal conditioners for the three force sensors.

The $\frac{1}{4}$-in.-diam shaft that was threaded through the center of gravity (c.g.) of the model passed through the ground plane and was constrained by two sets of bearings. Thus, the model was free to rotate about an axis that was perpendicular to the ground plane shown in Fig. 30 in the absence of the restraining force provided by the force sensor. The model, shaft, and bearings were allowed to move in the cross-stream direction, or to slide across the ground plane, as they were attached to a linear air bearing. The sled of this linear slide was in turn constrained in its motion by force sensors, as shown in Fig. 31, in which it can also be observed that the model was constrained from rotating by another force sensor and a moment arm. The projectile and the ground plane thus mimicked a projectile and actuator combination that was the half projectile used and its mirror image.

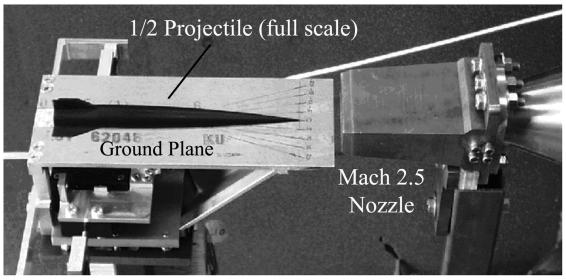


**Fig. 30 Top view of the half model setup.**

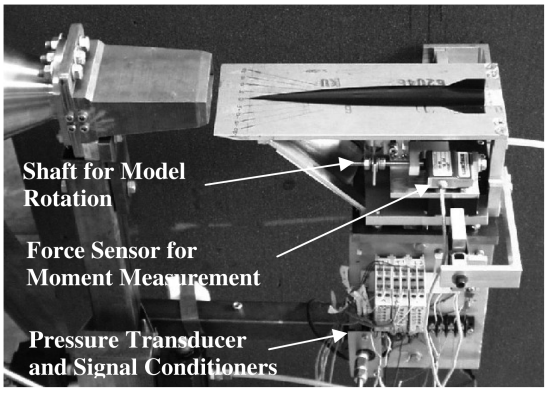


**Fig. 31 Instrumentation view of the half model.**

Thus, the actual forces and moments should double whereas the angles of attack should have a one-to-one correspondence.

There was some concern regarding how representative of an actual projectile flying through the air that these measurements using this testing arrangement would be. A shadowgraph system was thus used to visualize the flow downstream of the jet exit. Although the nozzle was designed to operate shock free at $M = 2.5$, it was found that the most shock-free condition was actually at $M = 2.475$ and thus, for all the measurements made, the jet was operated at this pressure ratio. However, when the projectile and ground plane were placed near the jet, additional flow disturbances were introduced. A location that introduced a weak shock off the leading edge of the ground plane yet forced the nozzle boundary layer to go below the ground plane was used and is shown in Fig. 32. This picture, which is not a shadowgraph, shows a shock introduced by the sharp leading edge of the ground plane. Although strong enough to be seen by the naked eye, this shock is nevertheless weak in the sense that the flow is only slightly affected. As seen at the bottom of Fig. 32, based on shock relations, the flow speed is reduced from $M = 2.475$ to 2.469, and the flow is turned to an angle of 0.3 deg. It was felt that this position of the ground plane introduced flow disturbances that could for the most part be neglected and thus, all measurements were made using this setup.

### B. Actuator Hardware

Based on the prior experiments with pins near a fin, it was decided to use a trapezoidal pin for the scale model tests. The pin was constructed out of aluminum and designed so that it would be flush with the body of the projectile when retracted. To locate the pin on the projectile, a hole was cut into the projectile near the vertical fin and into this hole one of two guide sleeves was inserted. The boat tail section of the model projectile with one of the guide sleeves inserted is shown in Fig. 33. The first actuator used was a manually driven micropositioner. This positioner, when combined with the pin, sleeve, and mounting hardware was attached to the underside of the model. An exploded view of this assembly is shown in Fig. 34, in which one can see that the actuation of the slide moves the pin in and out of the sleeve. When mounted to the model and viewed from the rear, the assembly appears as shown in Fig. 35 when the pin is fully deployed. (Recall that the model mimics one half of a projectile, and there would be a mirror image actuator on the other side of the projectile.) The manually driven micropositioner actuator was used for the majority of the force and moment measurements as the position of the pin could be readily controlled in a repeatable and verifiable fashion.

### C. Experimental Results

Data was acquired for the half projectile model at a Mach number of 2.47 for projectile angles of attack ranging from 7 to −7 deg. For each measurement, the projectile was fixed at a given angle before the flow was turned on. The force and moment data from the three force sensors were captured using a data acquisition card and customized Labview software. Both the force and moment data were found to be stationary with time; thus, the data were typically averaged over a period of 1 s.

In the experimental setup used to acquire these results, the pin height was set manually using the linear positioner. Data were thus rapidly acquired for multiple pin heights for a range of projectile angles of attack. It was found that the side force produced increased with increasing pin height as expected. As shown in Fig. 36, the amount of force induced by the flow interactions due to the presence of the pin ranges from 1–2 lb for the largest pin height (3.3 mm). It is also seen that the force is larger as the AOA is increased (as the pin is on the windward side of the fin). The effect of the pin height on the moment is shown in Fig. 37, and these moments correspond to the forces assuming a moment arm of about 5 in. Here the differences in pin height are more pronounced, and it can be noted that a pin height of 1 mm produces very little moment. This is most likely due to the fact that the pin does not extend out of the boundary layer, which was

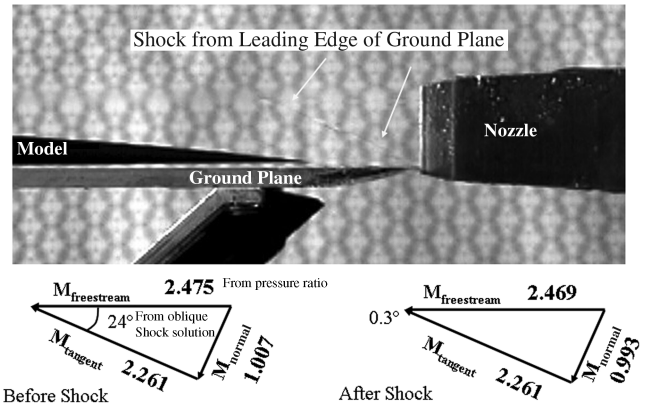


**Fig. 32 Shock introduced by the ground plane.**

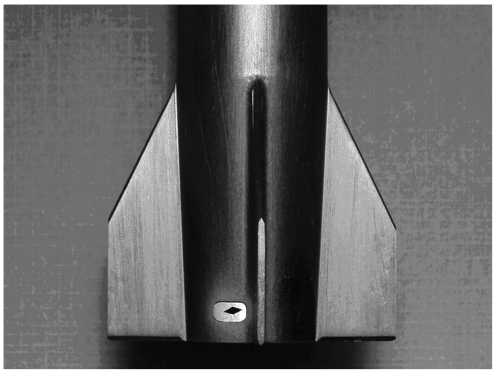

**Fig. 33 Pin AOA sleeve installed in the model.**

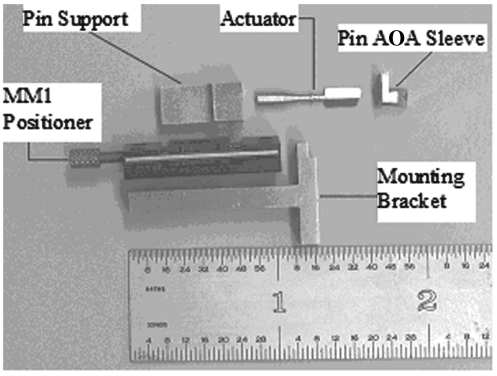


**Fig. 34 Exploded view of the actuator parts.**

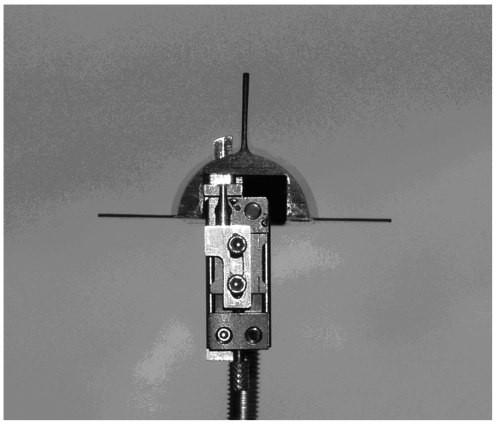

**Fig. 35 Actuator fully extended.**

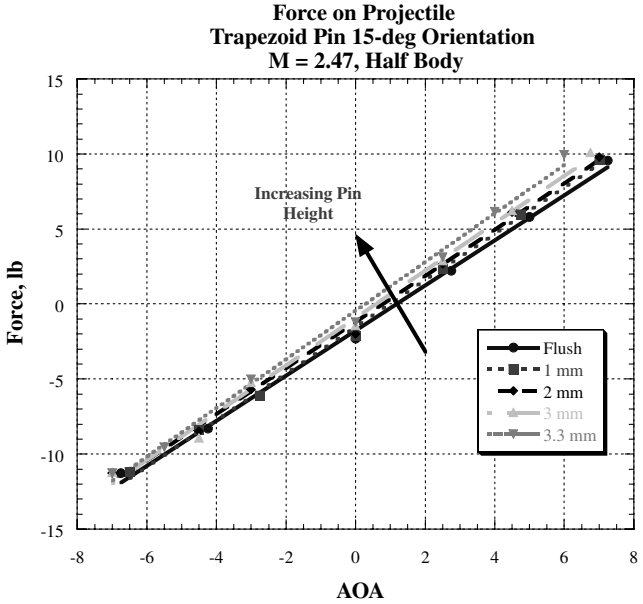


**Fig. 36 Experimentally measured forces on the half projectile for various pin heights.**

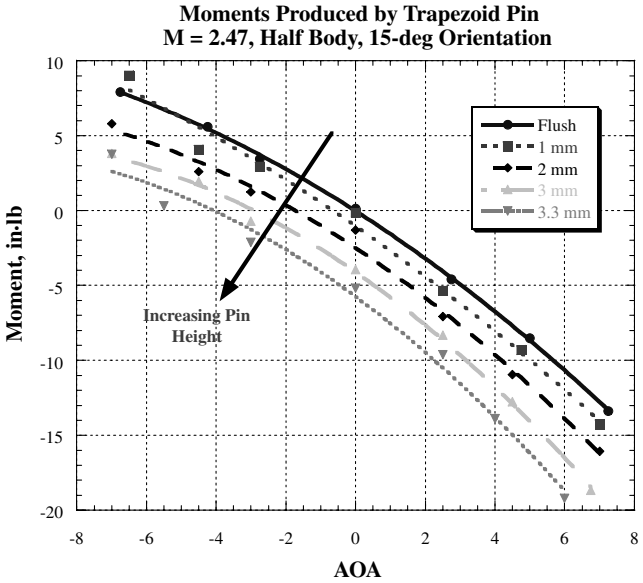


**Fig. 37 Experimentally measured moments on the half projectile for various pin heights.**

optically observed to be about 1.8 mm thick at this station. It is also observed that for a 3.3-mm insertion, enough moment is produced such that the restoring moment of the projectile is approximately equal to the moment produced by the pin at a 5-deg AOA. Thus, the pin at a 3.3-mm insertion should be able to rotate the projectile to about a 5-deg AOA.

## V. Guidance and Control with Pins or Jets

Using the experimental results, it was possible to estimate the forces that might be produced on a fin when a pin was deployed or a jet fired. Previous experimental and computational results also allowed for an estimation of the forces that might be produced on the body of a missile or projectile. Using these estimates, it was possible to consider several cases of controlling the flight of a missile or projectile.

The scheme most likely to be used for roll control would involve two diametrically opposed pins or jets, as shown in Fig. 26. Under the assumption that geometric similarity could be achieved in

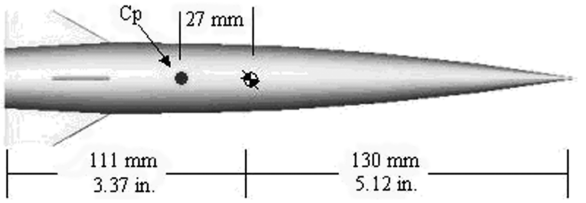


**Fig. 38 Projectile and the center of gravity location.**

manufacturing, the forces produced would result in a pure moment about the longitudinal axis of the body. The insertion depth of the pins or strength of the jets could be altered to increase or decrease the strength of the moment produced, thus providing control of the roll rate. Implementing a control of this type would also allow one to implement a bank to turn concept, which might result in a simpler control scheme than a projectile that was undergoing a constant spin. Without using the forces developed by placing the pins near the fins, roll control is not practical using actuators of these types as the pressure forces developed on the body do not introduce a rolling moment.

For directional control, a configuration in which the two pins are on the inside of adjacent fins was found to produce around 30 N of force on the projectile under consideration. The moment produced and the angle to which this forces the projectile depends upon several factors. The shape of the projectile and the fin area determines the center of pressure and the moment required to maintain an angle of attack. For this projectile, the c.p. location is shown in Fig. 38. The c.g. location is also shown in this figure. Both the moment produced by the pins and the baseline body aerodynamic moment depend on the location of the c.g. For the c.g. location shown in Fig. 38, the projectile is quite stable and the resulting moment from the pins would introduce about a 3-deg AOA. If the c.g. is shifted aft for a static margin of 8 mm, thus making the projectile less stable, the turn rate would be increased using the same steering moment from the pins.

These experiments have demonstrated the viability of using pin-based actuators for the guidance of supersonic fin stabilized rounds. It has been shown that the location of the pins is critical to generating the required forces, though some leeway exists. The geometry of the pin also affects the force generated, and it was shown that rectangular pins generate more force than round pins. Work remains on generating actuators that can be packaged into a projectile, though advances were made during the research, and a rocker pin concept has been developed that reduces the forces required to actuate the pins. It was also demonstrated that the pins could be made to actuate in a very short time and that there is no measurable lag in the rise of the aerodynamic forces. To achieve a 50-$g$ turn on the projectile under consideration with the reduced static margin, a mere 10.5 N of force is required to develop the 400 N of turning force required, as detailed in Table 1, which is nearly a 40:1 gain.

## VI. Conclusions

The proof of concept experiments and calculations described in this paper proved to be an important first step in a successful effort to demonstrate that a Mach 4 projectile could be steered with guidance pins. A series of experimental efforts demonstrated that pin in the corner flow of a fin could generate significant and tailorable forces on

**Table 1 Force gain of pin actuators (10.5 N input ⇒ 400 N guidance)**

| | |
|---|---|
| Force to deploy two pins | 10.5 N |
| Pin-induced force | 30 N |
| Moment arm | 0.11 m |
| Steering moment | 3.3 N · m |
| For a 50 $g$ turn | 400 N |
| AOA required | 7.1 deg |
| Static margin | 8 mm |

the fin. Further numerical simulations validated these results and also provided the corresponding pressures developed on the projectile body and the pin itself. From the CFD, it was possible to predict the rolling moments and pitching moments that could be developed by different pin configurations on a notional round. A second set of experiments was conducted using a wind-tunnel model, which demonstrated that a projectile would hold an angle of attack with pins deployed. Finally, estimates of the control authority and force amplification were made, and it was found that a supersonic projectile could be controlled using the guidance pins. Based on the success of these experiments, several additional phases of research were developed, and additional concepts for using the guided projectiles to defend against mortar threats have also been pursued by the U.S. Army.

With additional funding from DARPA, additional experiments were conducted to determine the pitch and roll rates as described by Silton [16], which were not measured in the aforementioned static experiments. These range tests on a subscale projectile demonstrated that the pins could be used to develop the required forces and further validated the forces and moments calculated from the prior experiments and CFD. Additional experiments were also conducted to further refine the location of the actuators and to develop pin deployment mechanisms as described by Hay and Massey [15]. A third phase of work was also sponsored by DARPA, in which test fires on the ARL Aeroballistic range [19] demonstrated the divert authority of the pin-based actuators.

## Acknowledgments

The authors would like to thank Sampath Palaniswamy at Metacomp, who was always a joy to work with on the CFD. We also appreciate the crew at ARL for many fruitful conversations and for helping out with the design of the projectile. This work was sponsored by DARPA.

## References

[1] Kandebo, S. W., "New Powerplant Key to Missile Demonstrator," *Aviation Week and Space Technology*, Vol. 157, No. 10, Sept. 2002, pp. 56–59.

[2] Marx, W. J., Wessling, F. C., III, Peters, B. R., Thies, A., Strickland, B. R., and Lianos, D., "Miniature Smart Munitions/Guided Projectiles for the Objective Force," *23rd Army Science Conference*, 2006.

[3] Warnash, A., and Killen, A., "Low Cost, High G, Micro Electro-Mechanical (MEMS), Inertial Measurements Unit (IMU) Program," *23rd Army Science Conference*, Dec. 2002.

[4] Margason, R. J., "Fifty Years of Jet in Cross Flow Research," AGARD, April 1993.

[5] Spaid, F. W., and Cassel, L. A., "Aerodynamic Interference Induced by Reaction Controls," AGARD, AD-775-209, Dec. 1973.

[6] Hemsch, M. J., *Tactical Missile Aerodynamics: General Topics*, Vol. 141, Progress in Astronautics and Aeronautics, edited by J. N. Nielsen, AIAA, New York, 1992.

[7] Hsia, H. T,-S,, "Equivalence of Secondary Injection to a Blunt Body in Supersonic Flow," *AIAA Journal*, Vol. 4, No. 10, Oct. 1966, pp. 1832–1834.

[8] Champigny, P., and Lacau, R. G.,"Lateral Jet Control for Tactical Missiles," AGAARD Special Course on Missile Aerodynamics, ONERA, June 1994.

[9] Schetz, J., "Effects of Pressure Mismatch on Slot Injection in Supersonic Flow," AIAA Paper 90-0092, Jan. 1990.

[10] Fujimori, T., "Numerical Prediction of Two and Three Dimensional Sonic Gas Transverse Injections into Supersonic Flow," AIAA Paper 91-0415, Jan. 1991.

[11] Takahashi, M., and Hayashi, A. K., "Numerical Study on Mixing and Combustion of Injecting Hydrogen Jet in a Supersonic Air Flow," AIAA Paper 91-0574, Jan. 1991.

[12] Edwards, J. A., "Concepts Behind the UK HOTLiP Maneuvering Projectile Program," AIAA Paper 2001-4317, Aug. 2001.

[13] Graham, M. J., and Weinacht, P., "Numerical Simulation of Lateral Control Jets," AIAA Paper 99-0510, Jan. 1999.

[14] Graham, M. J., Weinacht, P., and Brandeis, J., "A Numerical Investigation of Supersonic Jet Interaction for Finned Bodies," AIAA Paper 2000-0768, Jan. 2000.

[15] Hay, F., and Massey, K. C., "Parametric Investigation into the Location and Geometry of Deployable Pins Used for Guiding Supersonic Projectiles," AIAA Paper 05-2-20B, June 2005.

[16] Silton, S., "Comparison of Predicted Actuator Performance for Guidance of Supersonic Projectiles to Measured Range Data," AIAA Paper 2004-5195, Aug. 2004.

[17] Massey, K. C., Guthrie, K. B., and Silton, S. I., "Optimized Guidance of a Supersonic Projectile Using Pin Based Actuators," AIAA Paper 05-4966, June 2005.

[18] Massey, K. C., McMichael, J., Hay, F., and Warnock, T., "Mechanical Actuators for Guidance of a Supersonic Projectile," AIAA Paper 05-4970, June 2005.

[19] Massey, K. C., and Silton, S. I., "Testing the Maneuvering Performance of a Mach 4 Projectile," AIAA Paper 06-3649, June 2006.

M. Costello
*Associate Editor*